Design of large experimental facilities in heavy ion physics

... with focus on the MPD experiment at NICA ...

V. Riabov

System evolution in heavy-ion collisions

Fireball is ~10^{-15} meters across and lives for $5x10^{-23}$ seconds

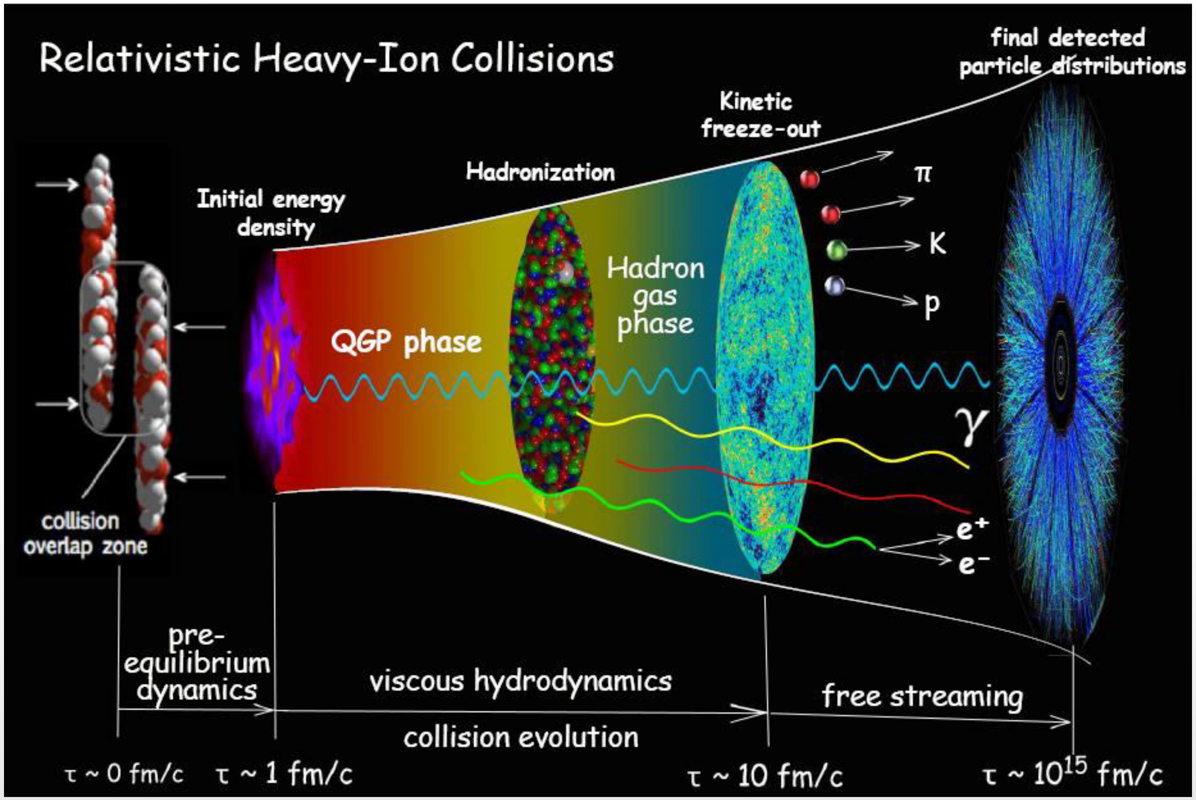

- The measurements are used to infer properties of the early state of relativistic heavy-ion collisions
- Only final state particles are measured in the detector: γ, $e^{\pm}$, $\mu^{\pm}$, π^0, $\pi^{\pm}$, K^0, $K^{\pm}$, η, ω, p, $\bar{p}$, ϕ, Λ, Σ, Ξ, etc.

Particle detection

- Only particles that interact with the detector materials or decay in particles that interact can be detected
- Four known fundamental forces: Gravity, Weak, Electromagnetic and Strong interactions:
  - ✓ pions, protons: strong, electromagnetic
  - ✓ photons, electrons, muons: electromagnetic
- Particle decays:
  - ✓ strong and electromagnetic decays → very small lifetimes, ~ 10^{-23} s → decay daughters are undistinguishable from primaries: $\pi^0(\eta) \rightarrow \gamma\gamma$, $\omega(\eta) \rightarrow \pi^0\gamma$ ($\pi^0 \pi^+ \pi^-$), $\rho \rightarrow \pi\pi$, $K^* \rightarrow \pi K$, $\phi \rightarrow KK$, etc.
  - ✓ weak decays → long lifetimes, ~ 10^{-10} s → secondary decay vertices can be separated: $K_s^0 \rightarrow \pi^0 \pi^0$, $K^\pm \rightarrow \mu\nu$, $\Lambda \rightarrow p\pi$, $\Sigma \rightarrow N\pi$, $\Omega \rightarrow \Lambda K$, etc.
- Detection of particles relies on the way particles (or daughters) interact with the materials:
  - ✓ track reconstruction in magnetic spectrometers → nondestructive method (particle remains): coordinates, momentum
  - ✓ calorimetric measurement of particle energy → destructive method (particle disappears): energy, coordinates
- Particle identification is an important ingredient of particle detection:
  - ✓ species dependent ionization losses: dE/dx vs. momentum
  - ✓ species dependent time of flight: Tof vs. momentum
  - ✓ species dependent shape of electromagnetic showers in the calorimeter: showers started by γ, $e^\pm$ and hadrons differ
  - ✓ species dependent penetration depth: $\mu^\pm$ can traverse a much larger width of material compared to other charged particles
  - ✓ species dependent threshold for Cherenkov/Transition radiation

Charged particle tracking

Magnetic field analysis

- Charged particles are bended in the external magnetic field

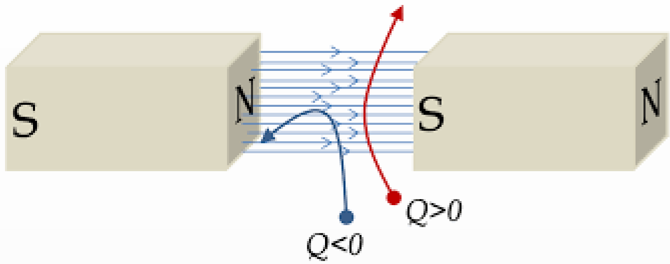

- The bending angle is related to particle momentum as p = q·B·R → for a fixed field B and particle charge q, the momentum p is proportional to the radius of curvature R
- Magnetic analysis is possible only for relatively long-lived particles to travel a measurable distance
- In nuclear physics, the relation becomes p [GeV/c] = 0.3 · B [T] · R [m] → a track with p = 1 GeV/c has a bending radius of R =1 m at B = 3T (magnetic field at the earth's surface is ~ $6 \cdot 10^{-5}$ T)
- Strong magnetic field and precise particle tracking can provide high resolution momentum measurements for long-lived charged particles
- Typical momentum resolution: $\delta p/p = \sqrt{c_1^2 + (c_2 p)^2}$ → less material and more precise tracking

  $\delta p/p = c_1$ for multiple scattering $\delta p/p = c_2 p$ for position resolution

- Gaseous and semiconductor (not covered) detectors are most often used to reconstruct charged particle tracks in large active areas/volumes → non-destructive measurements

Ionization and drift in gases

❖ Charged particles produce ionization:

Gas	Density, mg cm^{-3}	E_x eV	E_I eV	W_I eV	$dE/dx\|_{min}$ keV cm^{-1}	N_P cm^{-1}	N_T cm^{-1}
H_2	0.084	10.8	13.6	37	0.34	5.2	9.2
He	0.179	19.8	24.6	41.3	0.32	3.5	8
Ne	0.839	16.7	21.6	37	1.45	13	40
Ar	1.66	11.6	15.7	26	2.53	25	97
Xe	5.495	8.4	12.1	22	6.87	41	312
CH_4	0.667	8.8	12.6	30	1.61	28	54
C_2H_6	1.26	8.2	11.5	26	2.91	48	112
iC_4H_{10}	2.49	6.5	10.6	26	5.67	90	220
CO_2	1.84	7.0	13.8	34	3.35	35	100
CF_4	3.78	10.0	16.0	35-52	6.38	52-63	120

W_I - average energy for creation of ion pair
N_T - total number of electron-ion pairs per cm

❖ External electric field → force movement of electrons and ions in the opposite directions:

- ✓ Electron drift velocity v_e = f(P, T, E, mixture) → by measuring drift time one can reconstruct a drift length → coordinates of ionization area
- ✓ Electron cloud diffuses as it drifts, diffusion ~ $\sqrt{L}$ → dominates position resolution ~ $\sqrt{L}\,D_T/\sqrt{N}$
- ✓ Ion drift velocity v_i << v_e, linearly proportional to the electric field → can distort electric field configuration at high multiplicities/rates
- ✓ Gas mixtures are optimized for ionization density, drift velocity and spatial resolution (noble gases + quenchers)

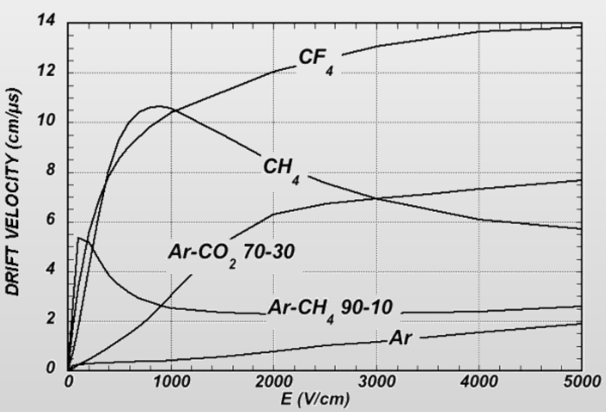

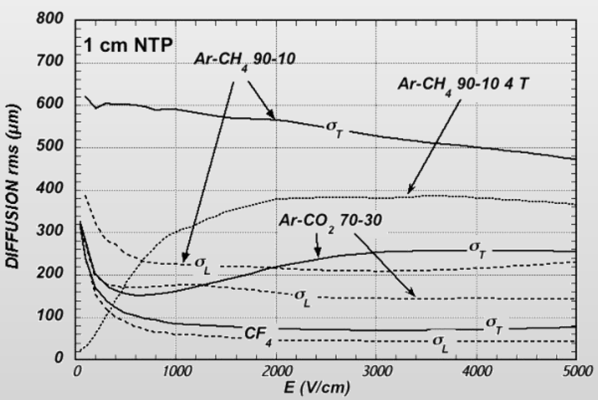

Ion mobility, $v_i \sim \mu E$

Gas	Mobility μ (cm^2 V^{-1} s^{-1})
He	10.4
Ne	4.7
Ar	1.54
Ar/CH_4	1.87
Ar/CO_2	1.72
CH_4	2.26
CO_2	1.09

Gas amplification

- If E >> 1 then electrons gain enough energy in a mean free path (λ) to ionize the gas
- $\alpha = 1/\lambda$ is the first Townsend coefficient
- Gas amplification (avalanche): $N = N_0 \cdot e^{\alpha x}$ in uniform electric field

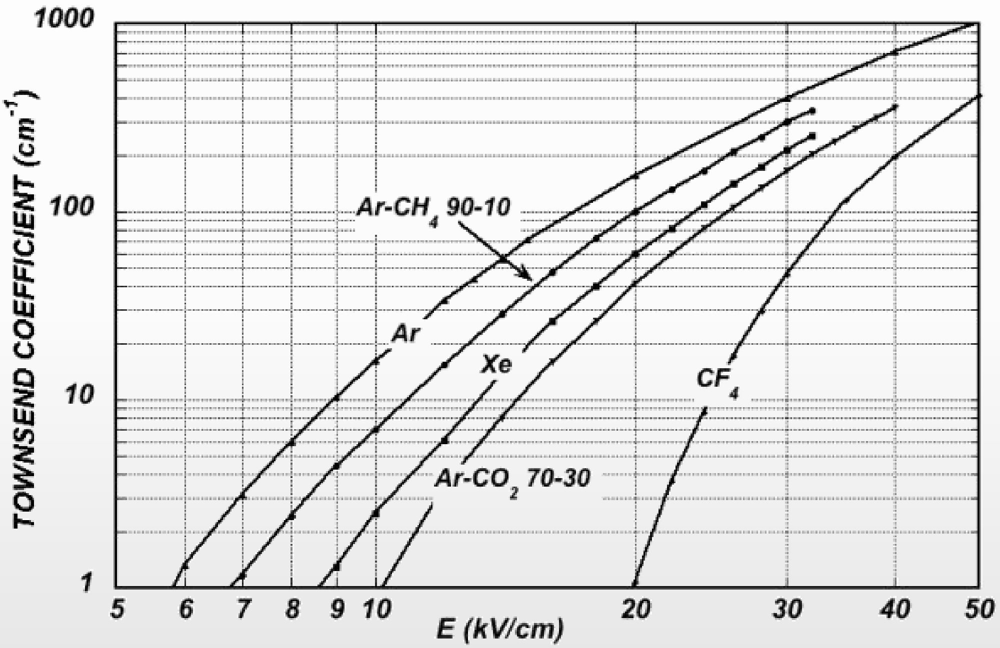

- Effective gas amplification starts at E > 20 kV/cm
- Large difference in threshold fields for entering the amplification regime for different gases
- Typical gas amplification in gaseous detectors ~ 10^4 to produce measurable signals

Charged particle tracker – Drift Chamber

- A long evolution of gaseous tracking detectors: Geiger-Muller counter → Proportional counter → (Multiwire) proportional chamber → Drift chamber (DC) and Time Projection Chamber (TPC)
- Drift chamber of the PHENIX experiment at RHIC:

Wire potentials: Uc = -4.5 kV, Ug = -1.6 kV, Ub = -2 kV, Us - grounded
Wire diameters: B, G, C ~ 100 μm, S ~ 25 μm

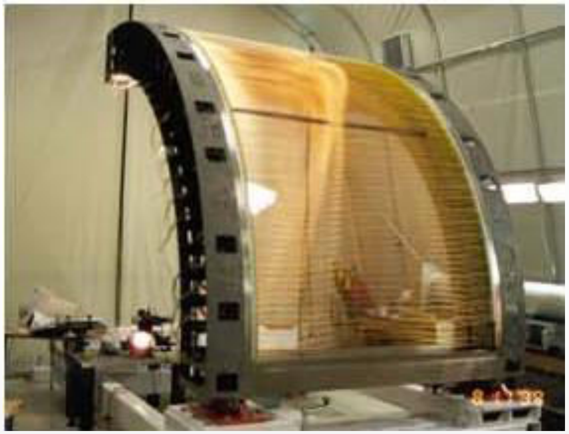

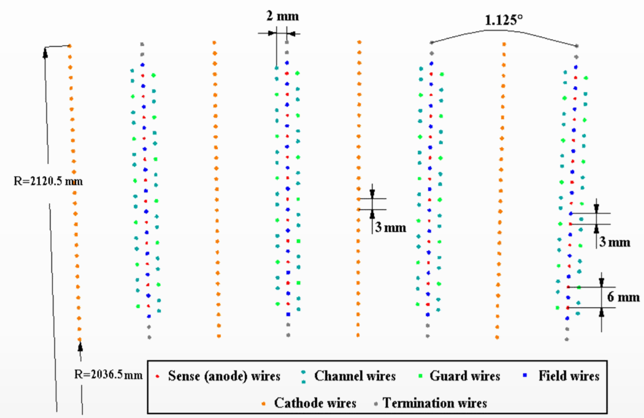

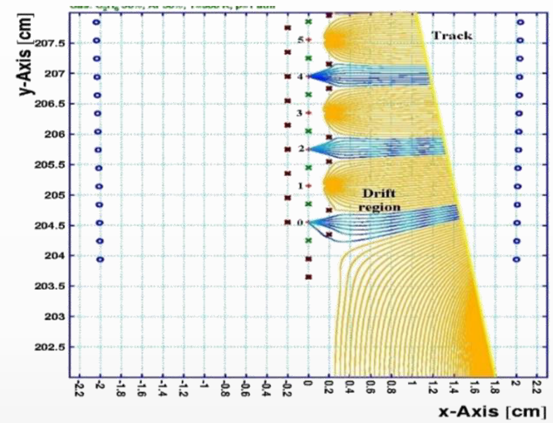

- ✓ Large gas volume of a few m^3 filled with specific gas mixtures to provide constant v_e and high GA: Ar-C_2H_6, 50%-50%
- ✓ Wires of different types and thickness have different voltages applied to produce required electric field configuration
- ✓ Charged particle produces electron-ion pairs along the path in the had mixture (Ar-C_2H_6, 50%-50%)
- ✓ Electrons drift towards the plane of sensitive (S) wires, v_e ~ 50 μm/ns → 2 cm drift in ~ 400 ns
- ✓ Drifting electrons are amplified next to S-wires in strong electric field (E ~ q/r)
- ✓ Measurable signal is detected on S-wires → drift time from the ionization region, T_d
- ✓ Drift time is converted to the drift distance, $L = v_e * T_d$ → one point in space (efficiency ~100%, resolution ~120μm)
- ✓ 10-20 points are measured along the path → track reconstruction → magnetic field analysis → $\delta p/p = \sqrt{(0.5\%)^2 + (1\% \cdot p)^2}$
- ✓ Double-track resolution ~ 1 cm

Gaseous trackers – Time Projection Chamber

❖ A typical Time Projection Chamber:

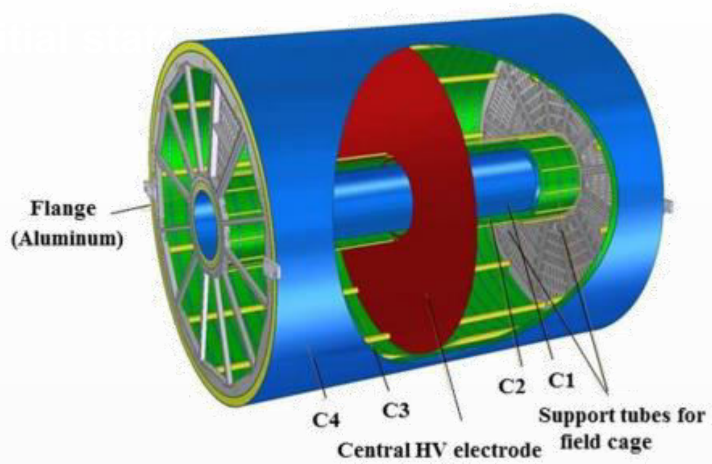

Item	Dimension
Length of the TPC	340 cm
Outer radius of vessel	140 cm
Inner radius of vessel	27 cm
Outer radius of the drift volume	133 cm
Inner radius of the drift volume	34 cm
Length of the drift volume	163 cm (of each half)
HV electrode	Membrane at the center of the TPC
Electric field strength	$\sim$ 140 V/cm
Magnetic field strength	0.5 Tesla
Drift gas	90% Ar+10% Methane, Atmospheric pres. + 2 mbar
Gas amplification factor	$\sim 10^4$
Drift velocity	5.45 cm/μs
Drift time	$<$ 30 μs

- ✓ A large volume detector: $|\Delta\varphi| < 2\pi$, L ~ 350 m, $R_{i/o}$ ~ 30/150 cm
- ✓ Uniform electric field is formed by the central membrane (~ 30 kV) and voltage dividers on the vessel walls / rods
- ✓ Charged particle produces electron-ion pairs along the path
- ✓ Electrons drift towards the side planes equipped with MWPC, v_e ~ 50 μm/ns → 150 cm drift in ~ 30 μs
- ✓ Reconstructed points in the MWPC produce 2D projection of track
- ✓ The measured drift time is converted to drift distance to add the third coordinate → 3D points along the tracks
- ✓ Up to 53 points are measured along the path → track reconstruction → magnetic field analysis → $^{\delta p}/_{p} = \sqrt{(1\%)^2+(1\%\cdot p)^2}$
- ✓ Double track resolution ~ 1 cm

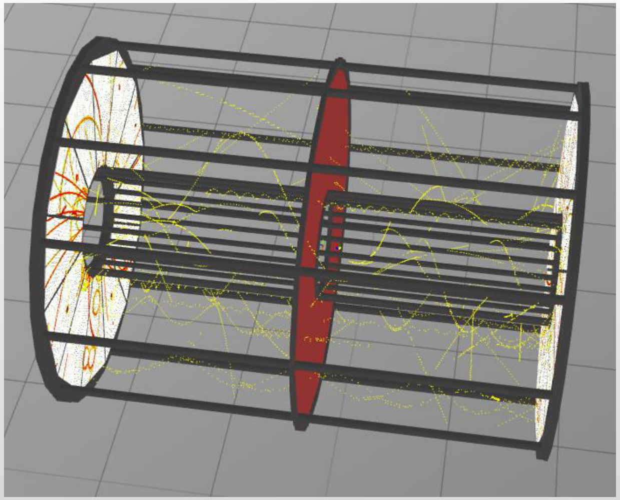

Application area of gaseous trackers

- Gaseous detectors are well suited to track charged particles in large active volumes (~ m^3)
  - ✓ high spatial resolution (~ 100 μm)
  - ✓ low material budget → minimize multiple scattering and photon conversion
  - ✓ sample many points along the track (10-200) → $\delta p/p \sim 1-2\ \%$
  - ✓ track hundreds and thousands of particles in a single event
  - ✓ small number of read-out channels (~ 10,000 - 100,000)
  - ✓ relatively cheap
  - ✓ PID by sampling particle dE/dx losses in the gas mixture

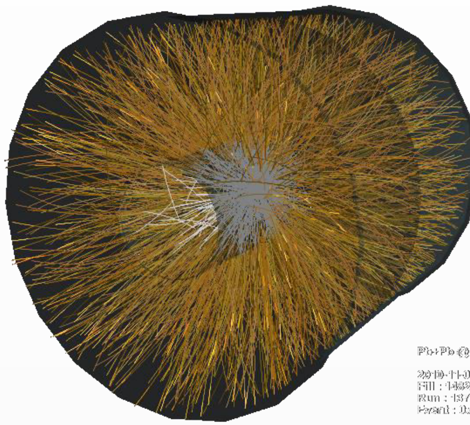

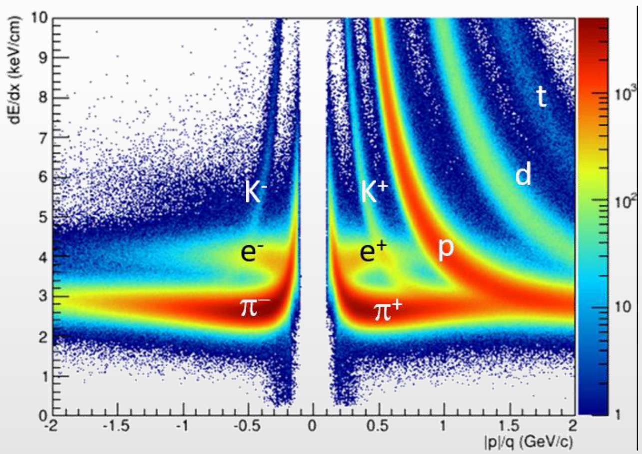

Bethe equation:

$$\left\langle -\frac{dE}{dx}\right\rangle = Kz^2\frac{Z}{A}\frac{1}{\beta^2}\left[\frac{1}{2}\ln\frac{2m_ec^2\beta^2\gamma^2W_{max}}{I^2}-\beta^2-\frac{\delta(\beta\gamma)}{2}\right]$$

valid at 0.1 < β < 1000 within a few percent

- ✓ z, β - charge and velocity of incident particle
- ✓ Z, A – atomic number and atomic mass of absorber
- ✓ W_{max} – maximum passible energy transfer
- ✓ I – mean excitation energy
- ✓ $\delta(\beta\gamma)$ - density effect correction

Stopping power in a given material is a function of beta alone

- Limitations:
  - ✓ relatively low event rate ~ 10-100 kHz
  - ✓ double track resolution of ~ 1 cm prevents effective tracking close to the event vertex
  - ✓ subject to ageing at high radiation loads

Further developments: Micro-Pattern Gas Detectors

- Position-sensitive detectors based on wire structures are limited by basic diffusion processes and space charge effects to localization accuracies of ~100 μm
- MPGD are developed to provide high rate capability (up to 10^6 Hz/mm^2) and excellent spatial resolution (down to 30 μm), large sensitive area and dynamic range and superior radiation hardness
- A broad family of MPGD technologies are being developed and optimized: Micro-Strip Gas Chamber (MSGC), Gas Electron Multiplier (GEM), Micro-Mesh Gaseous Structure (Micromegas), THick GEMs (THGEM), Resistive Plate WELL (RPWELL), GEM-derived architecture (μ-RWELL), Micro-Pixel Gas Chamber (μ-PIC), etc.

GEM (Gas Electron Multiplier)

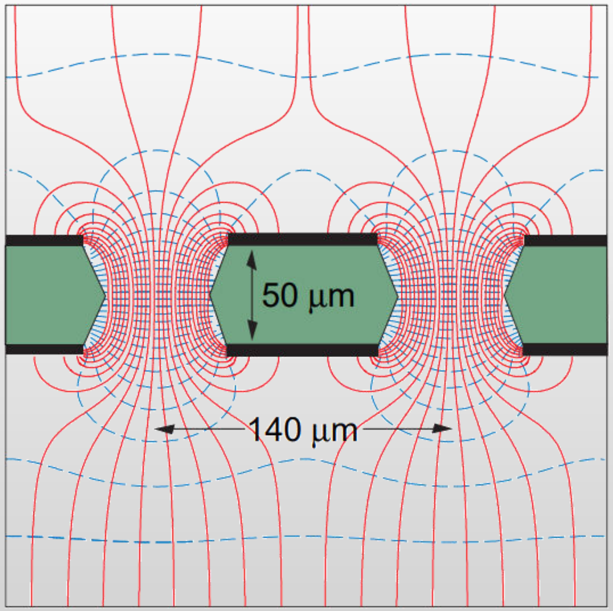

microMEGAS

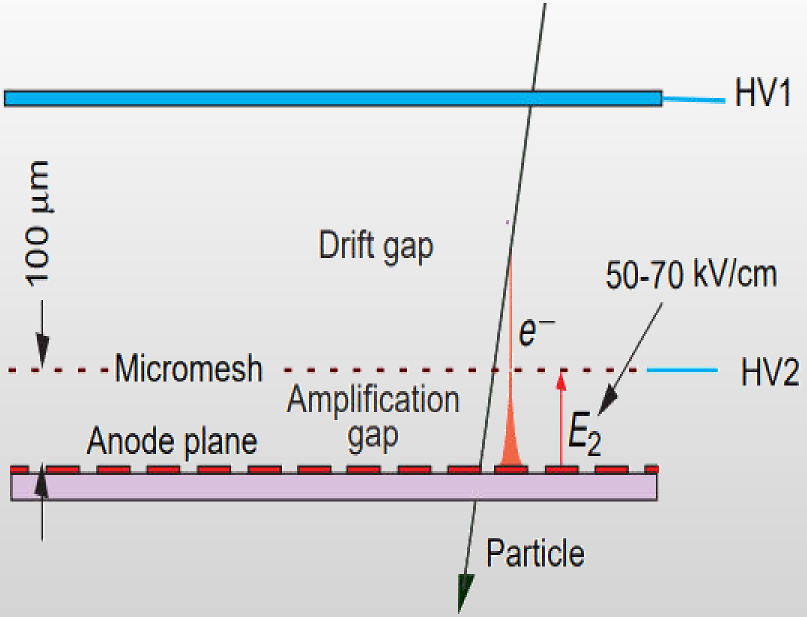

Initial state

QGP as a relativistic fluid

Calorimetry

Calorimeters

- Measure particle full energy → particle is absorbed → destructive method
- Vary by purpose → hadronic (not covered) and electromagnetic calorimeters
- Construction details:
  - ✓ Absorb full particle energy and be compact → materials with small radiation length (X_0), $E = E_0 \cdot e^{-L/X0}$

Material	X_0 [cm]	ρ_M [cm]	E_c [MeV]
Fe	1.76	1.77	21–27
Pb	0.56	1.60	7.4
U	0.32	1.00	6.8
W	0.35	0.92	8
Polystyrol	42.9	8.25	80–109
Ar	14	7.2	41.7
Si	9.36	5.28	37.6
BGO	1.12	2.33	10.2
H_2O	36.10	10.9	70

Electromagnetic calorimeter depth: 15-30 X_0
Hadronic calorimeter depth: 5-8 nuclear integration lengths

  - ✓ Not all absorbing material can provide signals → possible solutions:
    - crystal calorimeters (CsI, PbGl, $PbWO_4$) → best precision, very expensive
    - sampling calorimeters → bricks of absorber (Pb) and read-out materials (Sc) via WLS fibers

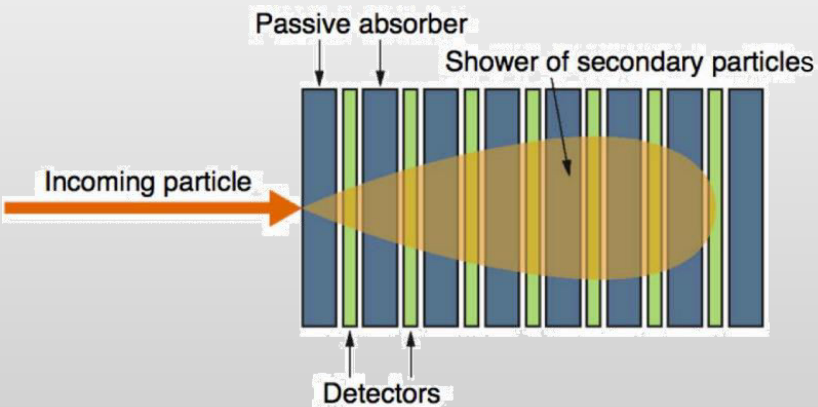

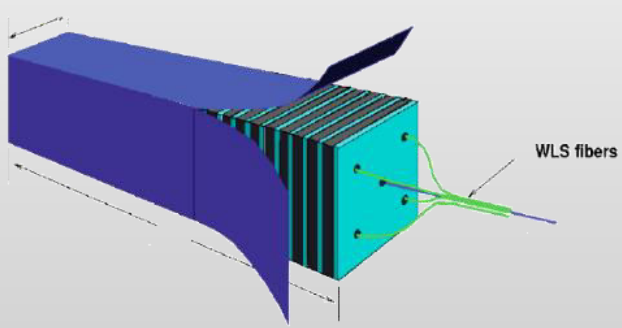

Calorimeter energy/spatial resolution

- The energy resolution of a calorimeter can be parameterized using:

$$\delta E/_{E} = \sqrt{c_1^2 + \left(\frac{c_2}{\sqrt{E}}\right)^2 + \left(\frac{c_3}{E}\right)^2}$$

calibration term $\delta E/_{E} \sim \text{const}$

statistical term $\delta E/_{E} \sim \delta N/_{N} \sim 1/_{\sqrt{N}} \sim 1/_{\sqrt{E}}$

noise term $\delta E/_{E} \sim const/_{E}$

Constant term dominates energy resolution at high energy

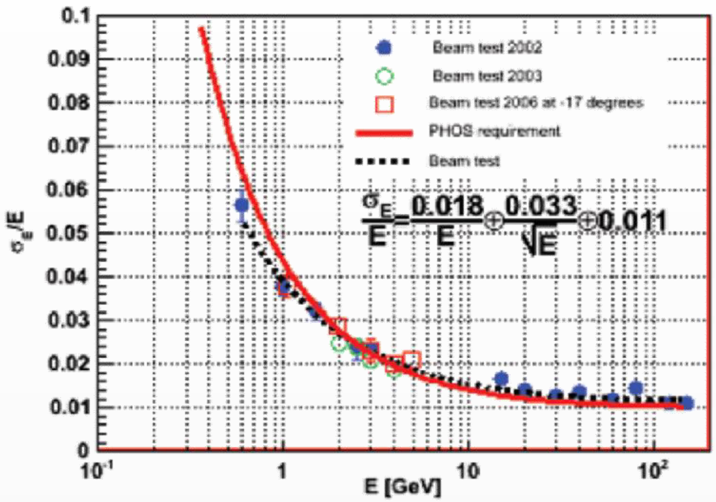

- Total signal is a sum of energies measured in several cells (towers) of the calorimeter → signal coordinates are weighted average of the tower coordinates

$$\bar{s} = \frac{\sum_{\text{digits}} s_i w_i}{\sum_{\text{digits}} w_i},$$

$$w_i = \max\left[0, p + \log\left(\frac{e_i}{E}\right)\right],$$

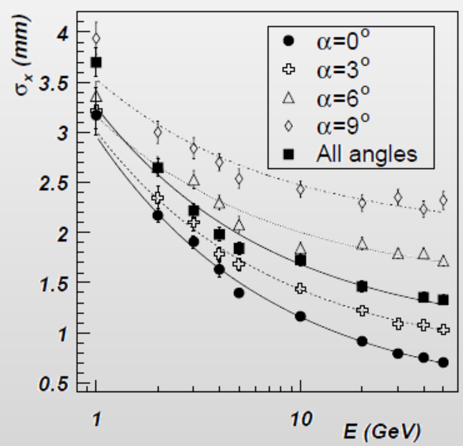

✓ Spatial resolution is inversely proportional to the measured energy, $\delta x/_{x} = \sqrt{c_1 + \frac{c_2}{E}}$

✓ At E → 0, spatial resolution tends to a half-size of a single calorimeter cell

- Both energy and spatial resolutions degrade at large incident angles → projective geometry is preferable

Shower shapes

❖ Shape and size of the energy deposition region depends on the particle species and type of interaction

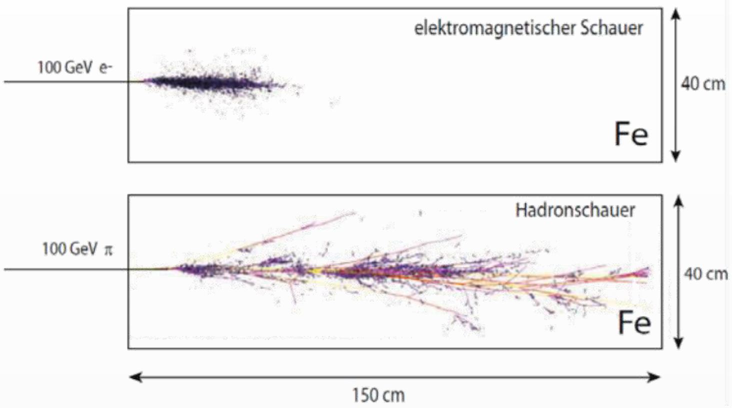

– Electromagnetic shower (γ, $e^{\pm}$)

– Production of mesons (π, K, …) and baryons (n, p, …)
– Spallation
– Excitation of nuclei
– Nuclear fission
– Photons from π^0 decays initiate new electromagnetic showers

❖ Shape of the electromagnetic shower can be measured ($e^{\pm}$ or photon beams) or simulated

❖ By comparing the measured and expected shower shapes one can discriminate between hadronic and electromagnetic showers → particle identification / hadron suppression:

$\text{Chi2} = \sum_i \frac{\left(E_i^{measured} - E_i^{expected}\right)^2}{\sigma_i^2}$, where: $E_i^{expected}$ is calculated for each tower based on the known shower shape, σ_i^2 is expected fluctuation of the energy distribution (empirical tuning), NDF – number of towers in the shower

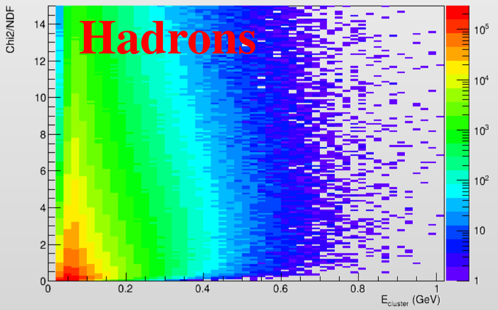

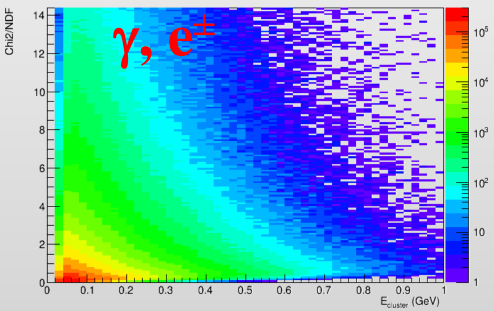

✓ shower shapes are different for (γ, $e^{\pm}$) and hadrons

✓ shower shape analysis is possible for showers with number of towers > 1

✓ provides capabilities for rejection of hadronic signals in the measurements for γ and $e^{\pm}$ → particle identification

Initial state

QGP as a relativistic fluid

Particle identification by velocity

Particle identification by time-of-flight (tof)

- Charged particle track is reconstructed in the tracking detector → magnetic analysis → momentum p
- Reconstructed track can be extrapolated to outer detector walls and matched to the measured hits
- Time of flight measurements are possible with fast detectors (MRPC, Micro channel plate detectors …)

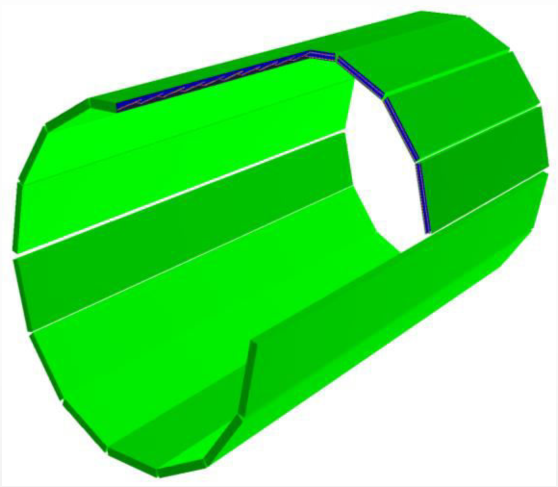

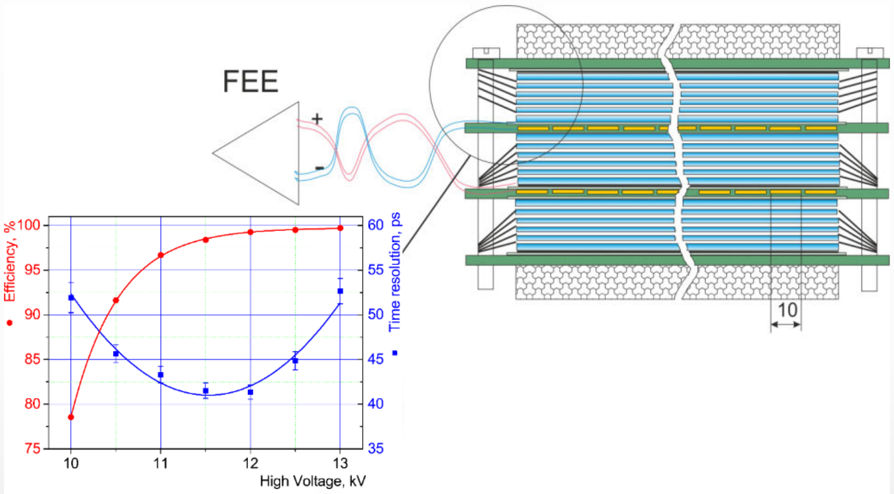

- Square of particle mass and the resolution are defined as:

$$m^2 = p^2\left(\frac{t^2c^2}{L^2} - 1\right) \qquad \delta^2_{m^2} = 4m^4\frac{(\delta p)^2}{p^2} + 4p^4\frac{tc}{L}\frac{(\delta t)^2}{t}$$

→ depends both on momentum and tof resolution
→ second term is inversely proportional to flight path L

- With momentum resolution of $\frac{\delta p}{p} \sim 1\%$ and $\delta t \sim 100$ ps charged hadrons are separated up to a few GeV/c

Complementary measurements

- Combined measurements of dE/dx and tof provide hadron separation in a wide momentum range:
  - ✓ tracker provides PID signals for all reconstructed tracks, including those with momentum → 0
  - ✓ TOF walls located at larger radii do not detect low-momentum particles (bend in the magnetic field)
- Both measurements are based on particle separation by velocity
- Particle separation from ~zero up to ~ 3 GeV/c

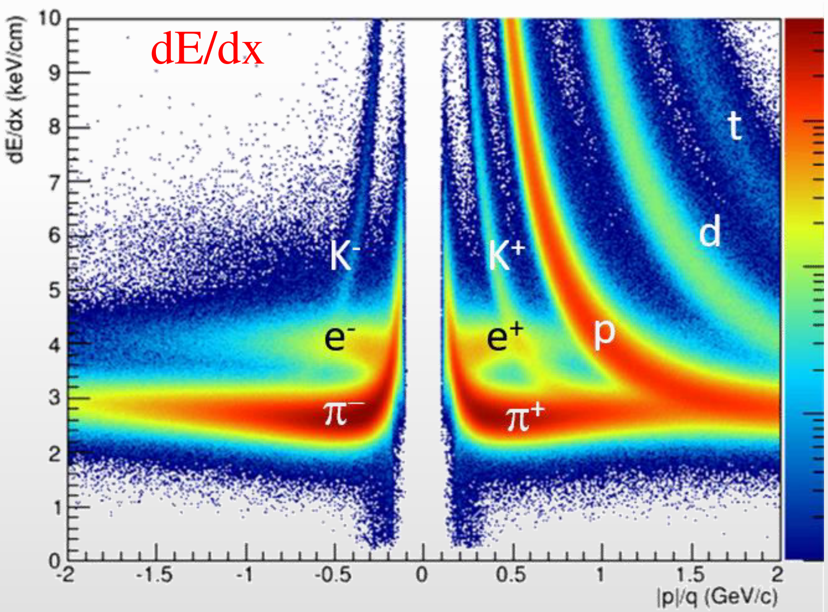

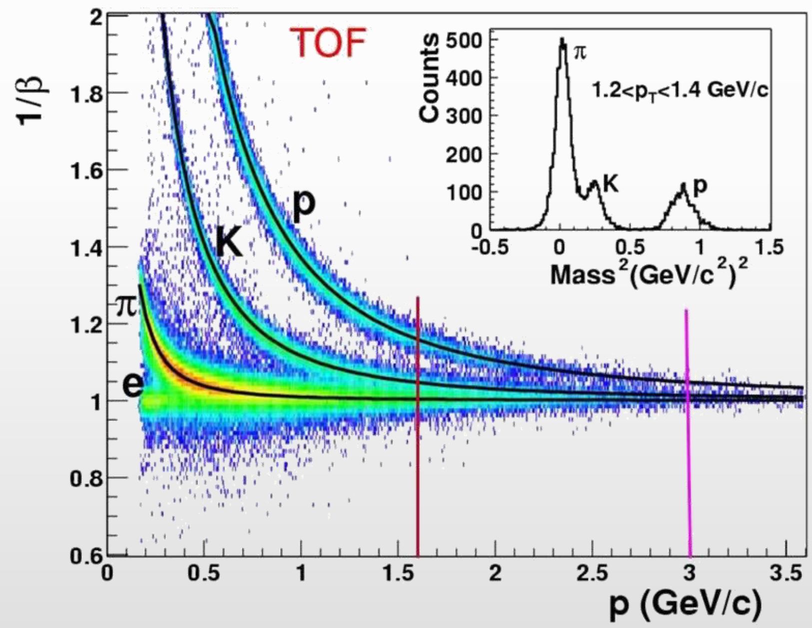

Cherenkov detectors

❖ Used as a threshold detector for electron identification and/or hadron identification at high momenta

❖ Cherenkov light is emitted along the particle trajectory if it moves faster than c/n, n – refraction index

$$\cos(\theta_c) = \frac{1}{n\beta}$$

- ✓ Threshold detector, v > c/n
- ✓ Light emitted at constant angle θ_c along the particle path make a circle on the read-out plane → Ring Imaging Cherenkov Detector (RICH)
- ✓ Particle velocity β defines circle radius → separation up to tens of GeV/c

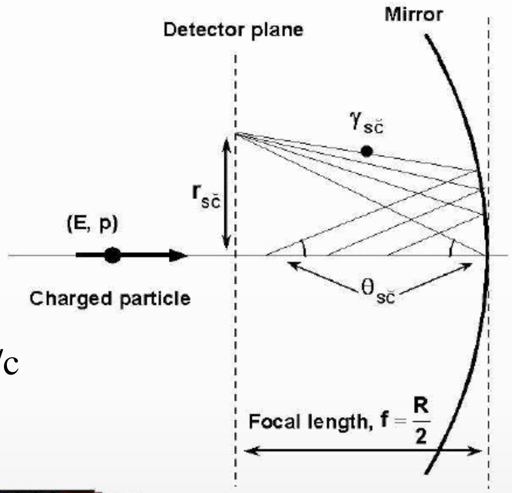

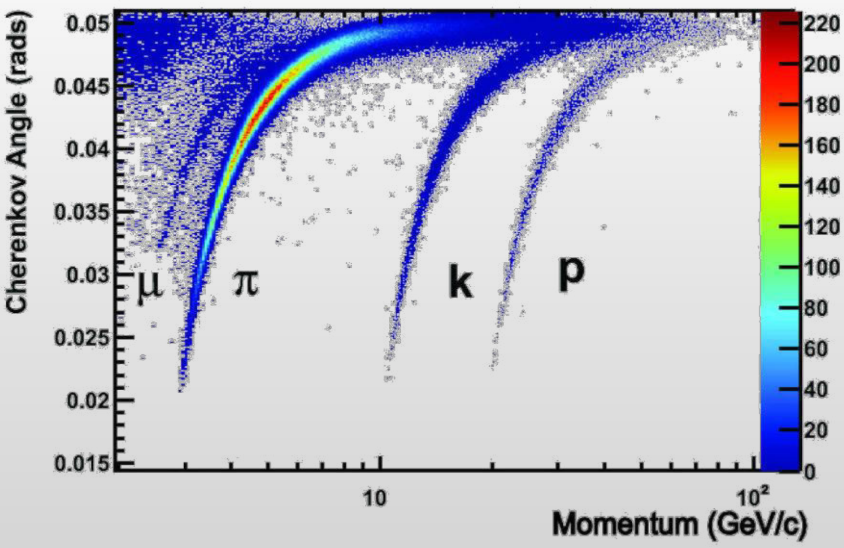

Initial state

QGP as a
relativistic
fluid

Heavy ion collisions at NICA

Operation details

- Relatively low collision energies (4-11 GeV):
  - ✓ modest multiplicity (~ 1000 particles per event)
    → modest track density even close to event vertex
  - ✓ bulk of particles is produced at low momentum ($\langle p_T \rangle$ ~ 100-300 MeV/c for light-flavor hadrons)
    → no need for a very strong magnetic field and high-momentum PID
  - ✓ heavy flavor production cross section is small
    → topic needs special attention

- Top NICA luminosity for heavy-ion beams is 10^{27} $cm^{-1}s^{-1}$:
  - ✓ maximum event rate ~ 7 kHz
    → no need for very fast detectors

Multi-Purpose Detector

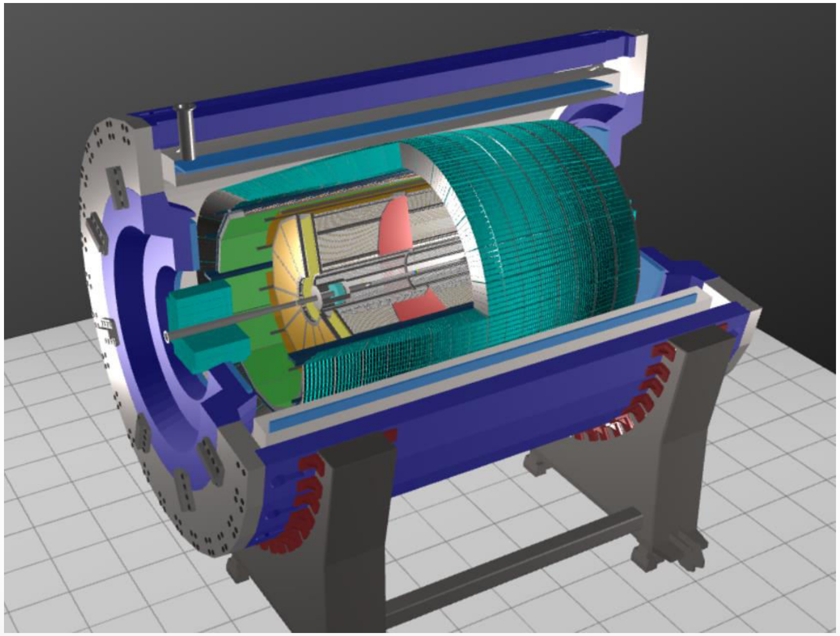

Length	340 cm
Vessel outer radius	140 cm
Vessel inner radius	27 cm
Default magnetic field	0.5 T
Drift gas mixture	90% Ar+10% CH_4
Maximum event rate	7 kHz ($L = 10^{27}$ $cm^{-2}s^{-1}$)

TPC: $|\Delta\varphi| < 2\pi$, $|\eta| \leq 1.6$

TOF, EMC: $|\Delta\varphi| < 2\pi$, $|\eta| \leq 1.4$

FFD: $|\Delta\varphi| < 2\pi$, $2.9 < |\eta| < 3.3$

FHCAL: $|\Delta\varphi| < 2\pi$, $2 < |\eta| < 5$

TPC: charged particle tracking + momentum measurements + identification by dE/dx

TOF: charged particle identification by m^2/β

EMC: energy and PID for $\gamma/e^{\pm}$ + charged particle identification (limited ability)

FFD/FHCAL: event triggering, event geometry, T_0

ITS: secondary vertex reconstruction for heavy-flavor decays (very small S/B ratio)

Charged particle tracking and PID

- Magnetic field ~ 0.5 T and up to 53 points measured along the track in the TPC:

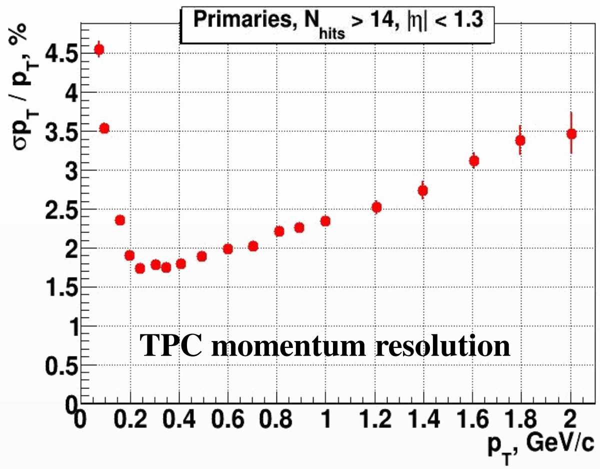

- PID by dE/dx (resolution ~6.5%) and tof (δt ~ 85 ps) → excellent light flavor hadron and fragment identification capabilities in a wide rapidity range

dE/dx vs momentum in TPC

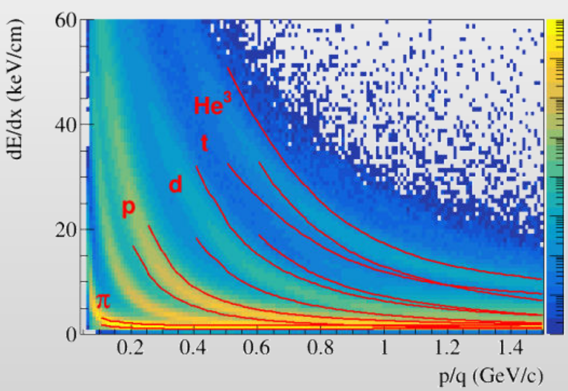

m^2 vs. momentum in TOF

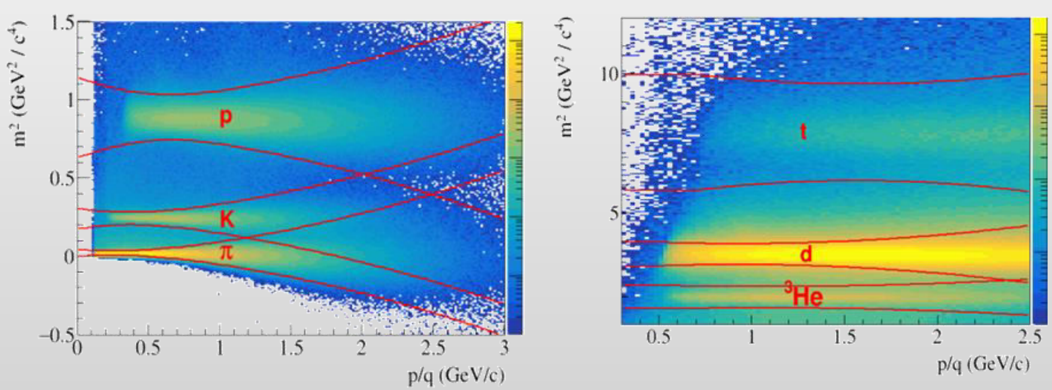

Electron identification

- ❖ Electrons are produced at low rates, $e/\pi \sim 10^{-3}$-10^{-4}
- ❖ Identification of electrons requires special treatment using capabilities of different detectors

TPC: log(dE/dx)

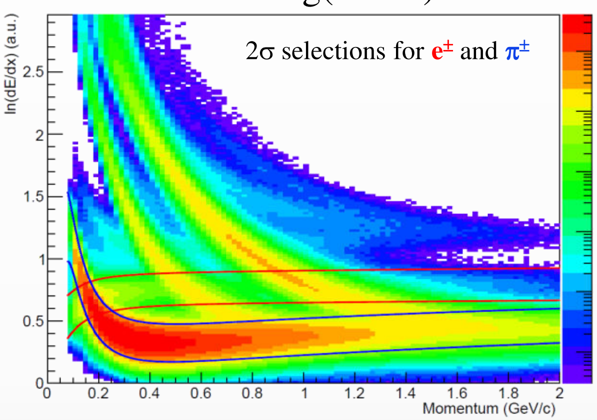

- ✓ eID at low momentum
- ✓ $e^{\pm}$ and $\pi^{\pm}$ bands merge at ~ 200 MeV/c

TOF: $\beta \sim 1$, $p_T > 150$ MeV/c

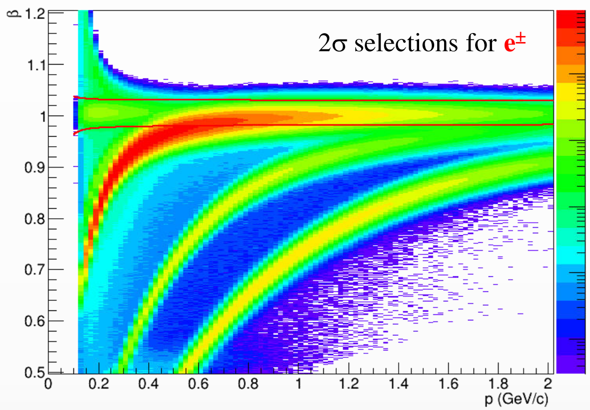

- ✓ $e^{\pm}$ with $p_T < 150$ MeV/c miss the TOF
- ✓ $e^{\pm}$ and $\pi^{\pm}$ bands merge at ~ 400 MeV/c

ECAL: tof < 2 ns ($\delta \sim 500$ ps) + $E/p \sim 1$

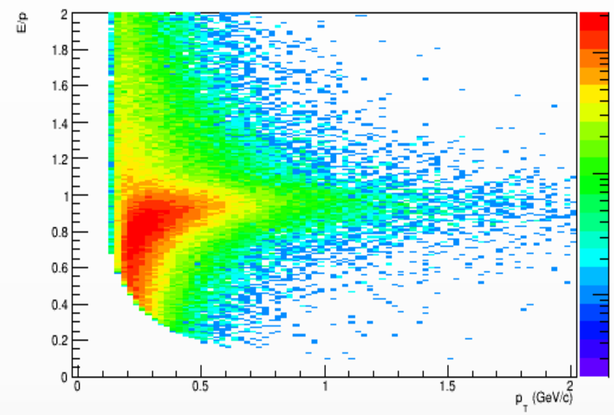

- ✓ $e^{\pm}$ with $p_T < 200$ MeV/c miss the ECAL
- ✓ $E/p \sim 1$ for $e^{\pm}$ at $p_T > 300$-400 MeV/c

- ❖ Each of the detectors provides more efficient electron identification in a limited range of momenta
- ❖ Combined use of the TPC-TOF-ECAL signals enhances the probability for a selected track to be true $e^{\pm}$

Electron efficiency and purity

- Simulated BiBi@9.2 GeV, realistic vertex distribution
- Selected tracks:
  - ✓ hits > 39
  - ✓ |η| < 1
  - ✓ |DCA_x,y,z| < 3 σ
  - ✓ 2σ matching to TOF
  - ✓ 1-2σ TPC-eID
  - ✓ 2σ TOF-eID

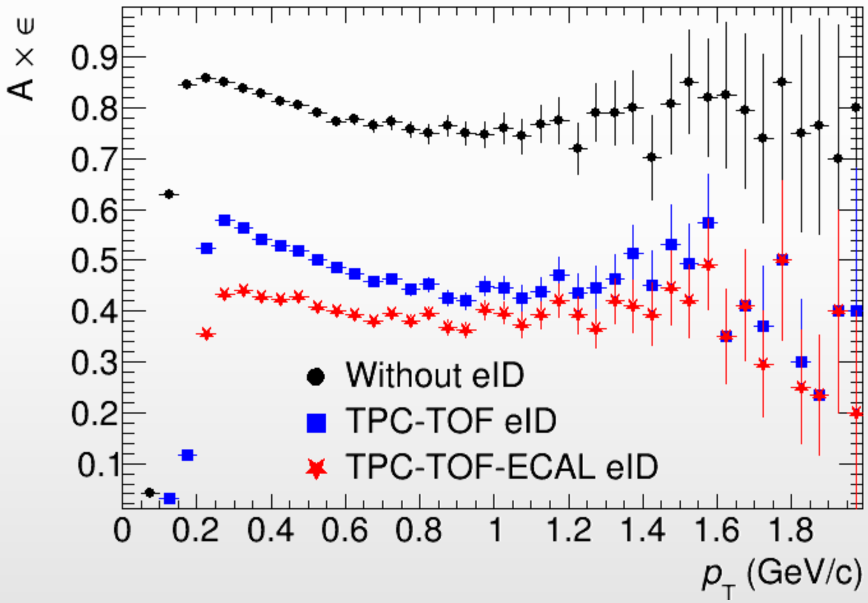

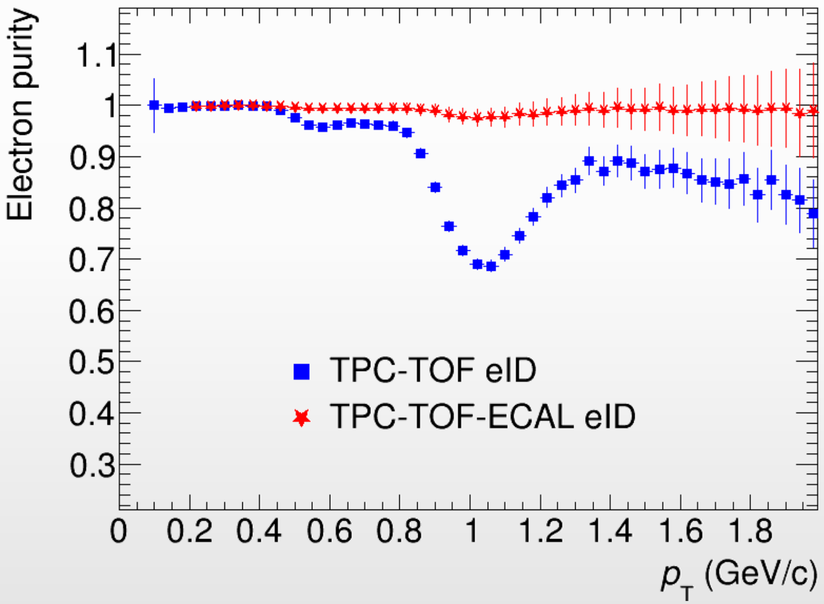

- Purity of ~ 100% at 40% reconstruction efficiency can be achieved at p_T > 150 MeV/c

Measurement of photons

- Photons can be measured in the ECAL or in the tracking system as e^+e^- conversion pairs (PCM):

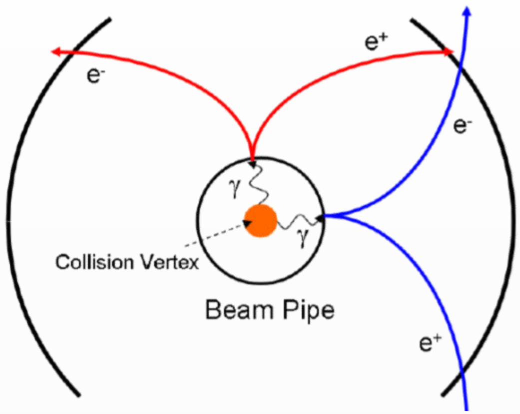

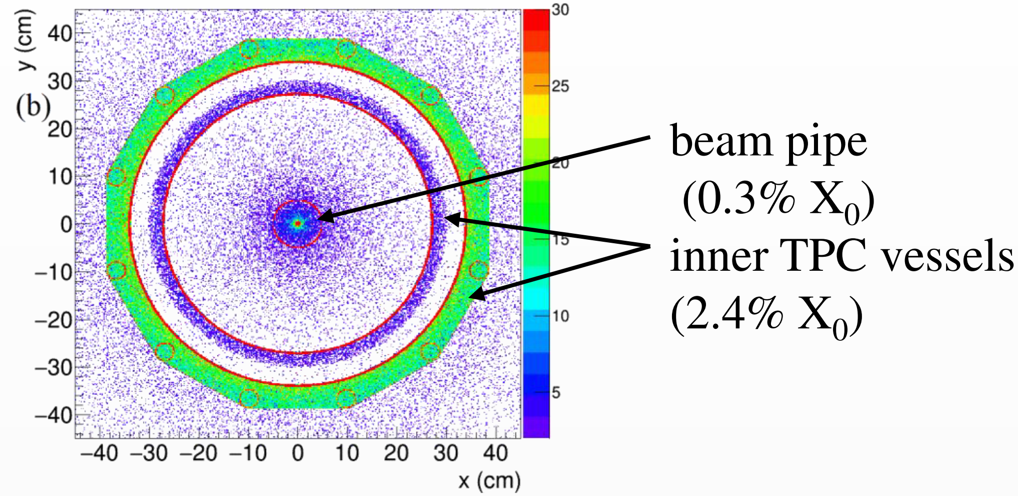

- PCM disadvantages: ~4% of photons convert, ~ 1.5% of photons is reconstructed (vs. ~ 60% in ECAL)
- PCM advantages: superior energy resolution and photon purity

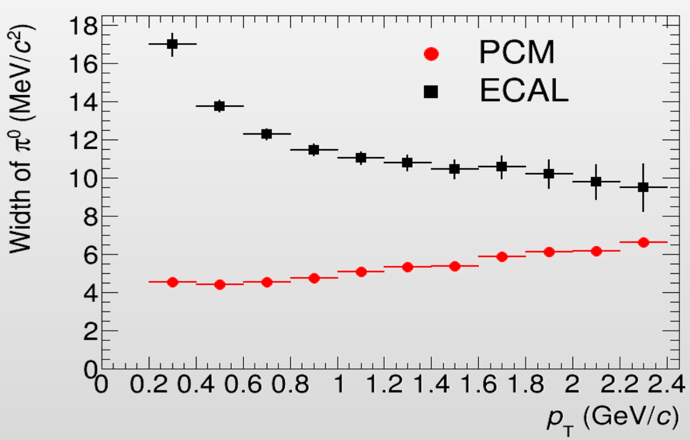

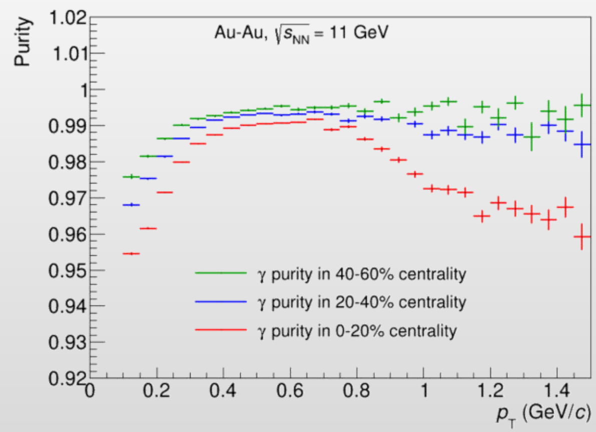

Reconstruction of neutral mesons

- Wide variety of neutral mesons:
  - ✓ π^0 ($\pi^0 \rightarrow \gamma\gamma$)
  - ✓ η ($\eta \rightarrow \gamma\gamma$, $\eta \rightarrow \pi^0 \pi^+ \pi$)
  - ✓ K_s ($K_s \rightarrow \pi^0 \pi^0$)
  - ✓ ω ($\omega \rightarrow \pi^0 \gamma$, $\omega \rightarrow \pi^0 \pi^+ \pi$)
  - ✓ η' ($\eta' \rightarrow \eta \pi^+ \pi$)

- Examples of π^0 reconstruction in the ECAL in two p_T intervals → measurable signals from 100 MeV/c:

0.1-0.2 GeV/c

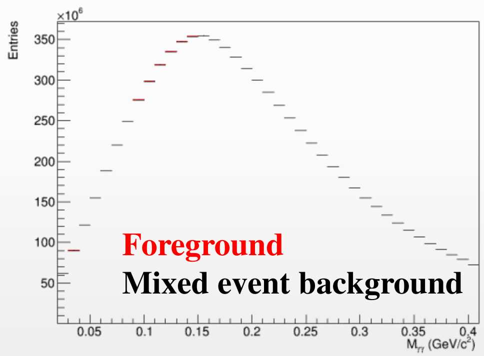

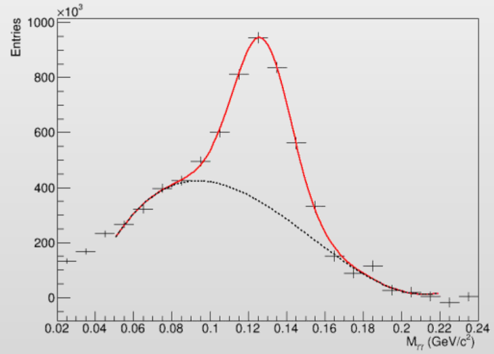

3-10 GeV/c

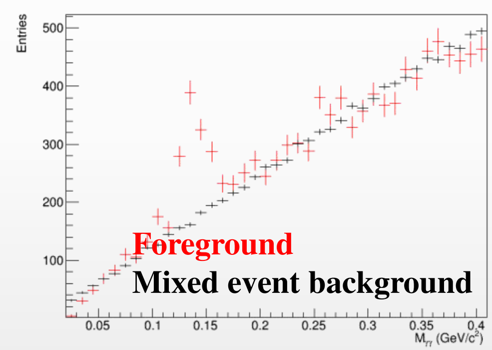

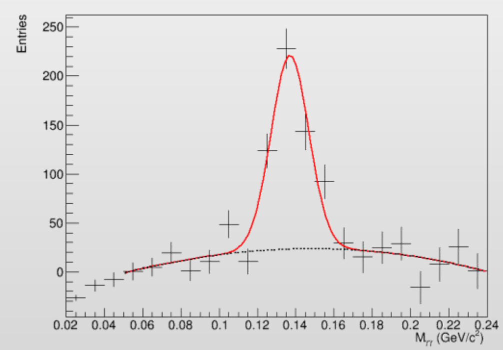

Summary

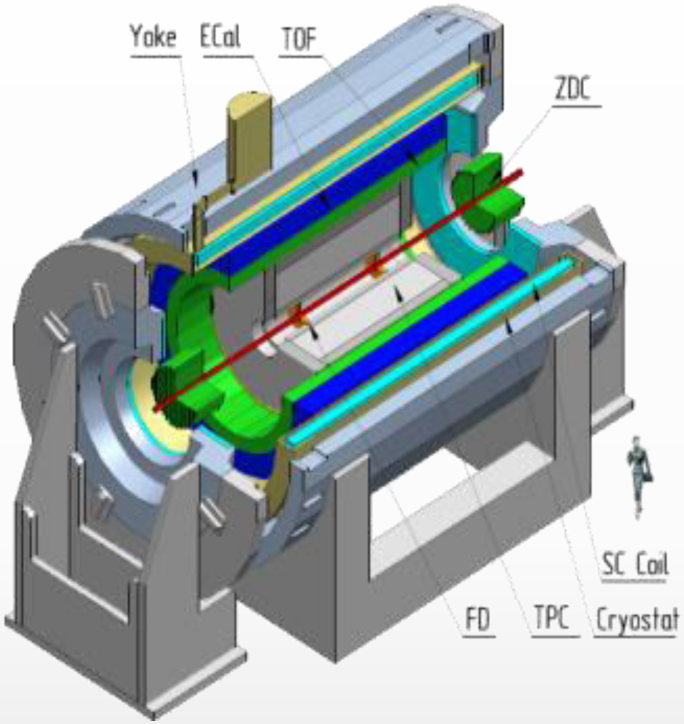

- Design of high energy heavy-ion experiments is driven by physics programs and accelerators
- For the MPD detector at NICA, well known detector technologies were selected to fulfill the requirements for the event rates and observables of interest at reasonable cost
- Relatively 'simple' design of the MPD detector provides high flexibility and physics potential
- The MPD detector is in final stage of production, commissioning and first data taking in 2025

BACKUP

Heavy-ion collisions

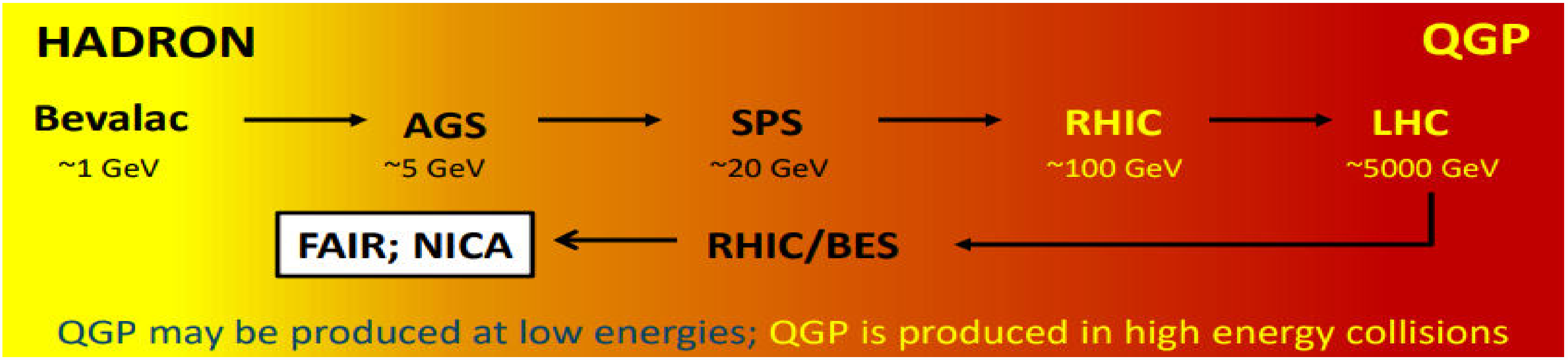

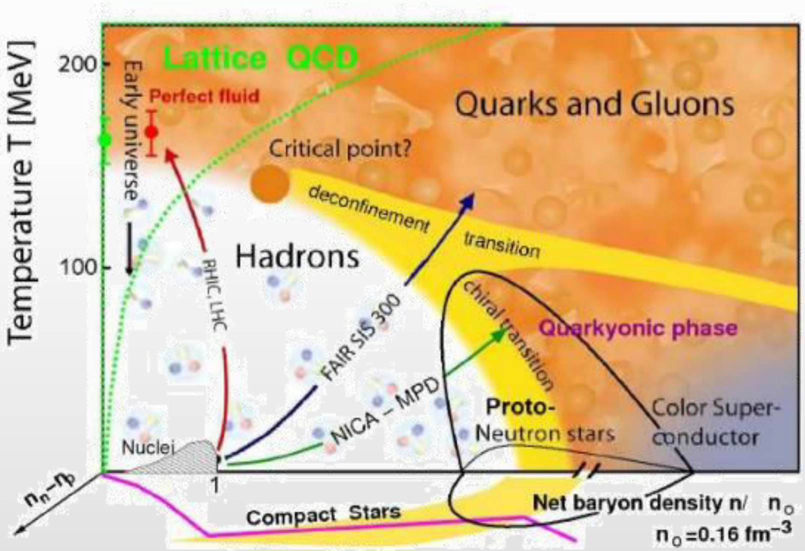

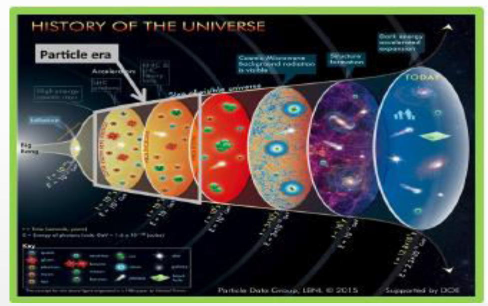

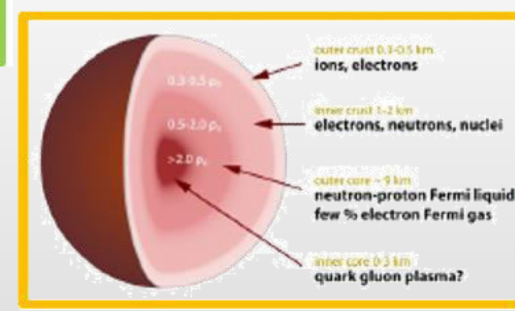

- Heavy-ion collisions are used to map the QCD phase diagram in different ranges of T and μ_B
- Probe conditions that existed during the first microseconds after the Big Bang or may exist in cores of compact neutron stars or in neutron star mergers

Calorimeter time resolution

- Intrinsic time resolution of calorimeters is ~ $100\ ps/\sqrt{E\ [GeV]}$ or better
- Experimental time resolution is driven by electronics performance, typical time resolution of modern calorimeters is ~ $500\ ps/\sqrt{E\ [GeV]}$
- Time-of-flight measurements with the calorimeters provide:
  - ✓ modest PID capabilities for hadrons
  - ✓ identification of photons, especially at low E where alternative PID techniques are not effective
    - photons travel along straight lines with speed of light → minimum time of flight
    - charged hadrons travel along bended trajectories (longer path) and with velocities << c → larger time of flight
    - the larger the distance from the event vertex the better is the separation between photons and hadrons in time of flight

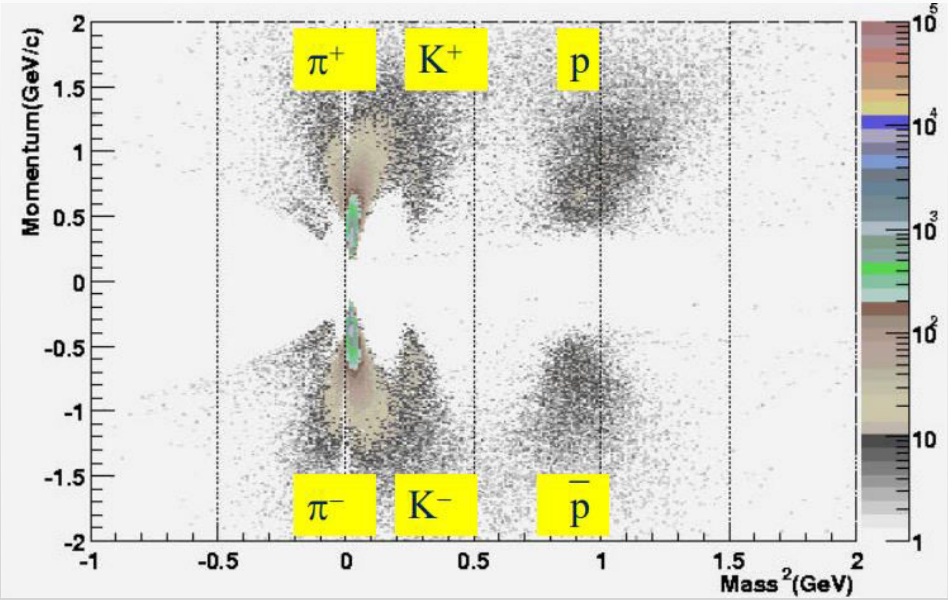

Short-lived resonances

- Resonances can not be directly detected → reconstructed using hadronic decay channels

increasing lifetime ⟶

	ρ(770)	K*(892)	Σ(1385)	Λ(1520)	Ξ(1530)	ϕ(1020)
cτ (fm/c)	1.3	4.2	5.5	12.7	21.7	46.2
$\sigma_{rescatt}$	$\sigma_\pi\sigma_\pi$	$\sigma_\pi\sigma_K$	$\sigma_\pi\sigma_\Lambda$	$\sigma_K\sigma_p$	$\sigma_\pi\sigma_\Xi$	$\sigma_K\sigma_K$

- BiBi@9.2 GeV (UrQMD) after mixed-event background subtraction: *Phys.Scripta* 96 (2021) 6, 064002

$\phi(1020) \to K^+K^-$

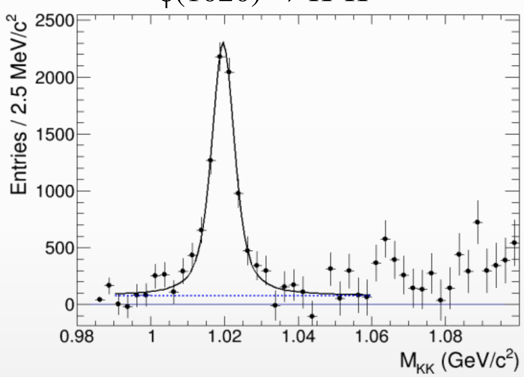

$K^*(892)^\pm \to \pi^\pm K_s$ ($K_s \to \pi^+\pi^+$)

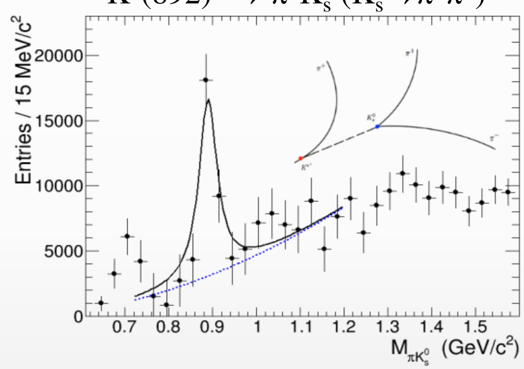

$\Sigma(1385)^\pm \to \pi^\pm\Lambda$ ($\Lambda \to p\pi$)

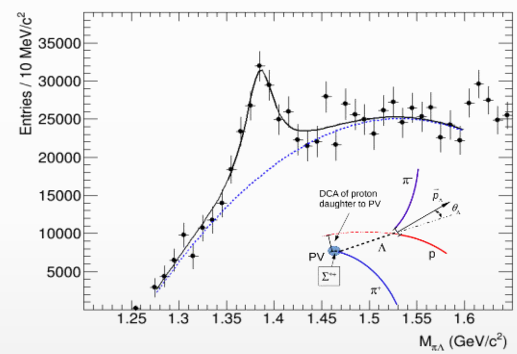

$\Lambda(1520) \to pK^-$

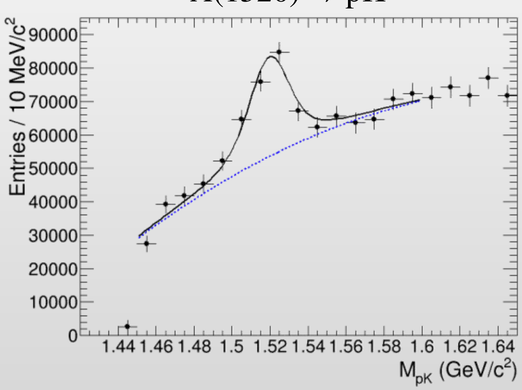

$\Xi(1530)^0 \to \pi^+\Xi^-$ ($\Xi^- \to \Lambda\pi^-$, ($\Lambda \to p\,\pi^-$))

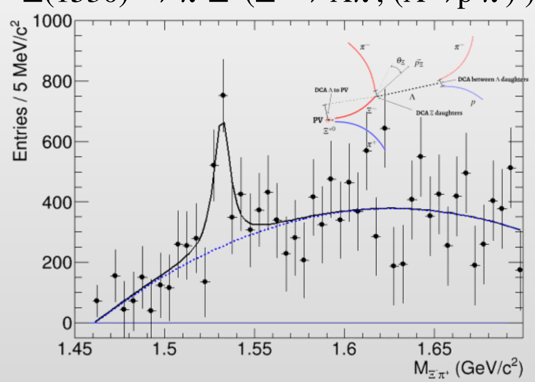

✓ MPD is capable of reconstruction the resonance peaks in the invariant mass distributions using combined charged hadron identification in the TPC and TOF

✓ decays with weakly decaying daughters require additional second vertex and topology cuts for reconstruction

Hyperon reconstruction

- BiBi@9.2 GeV (UrQMD)

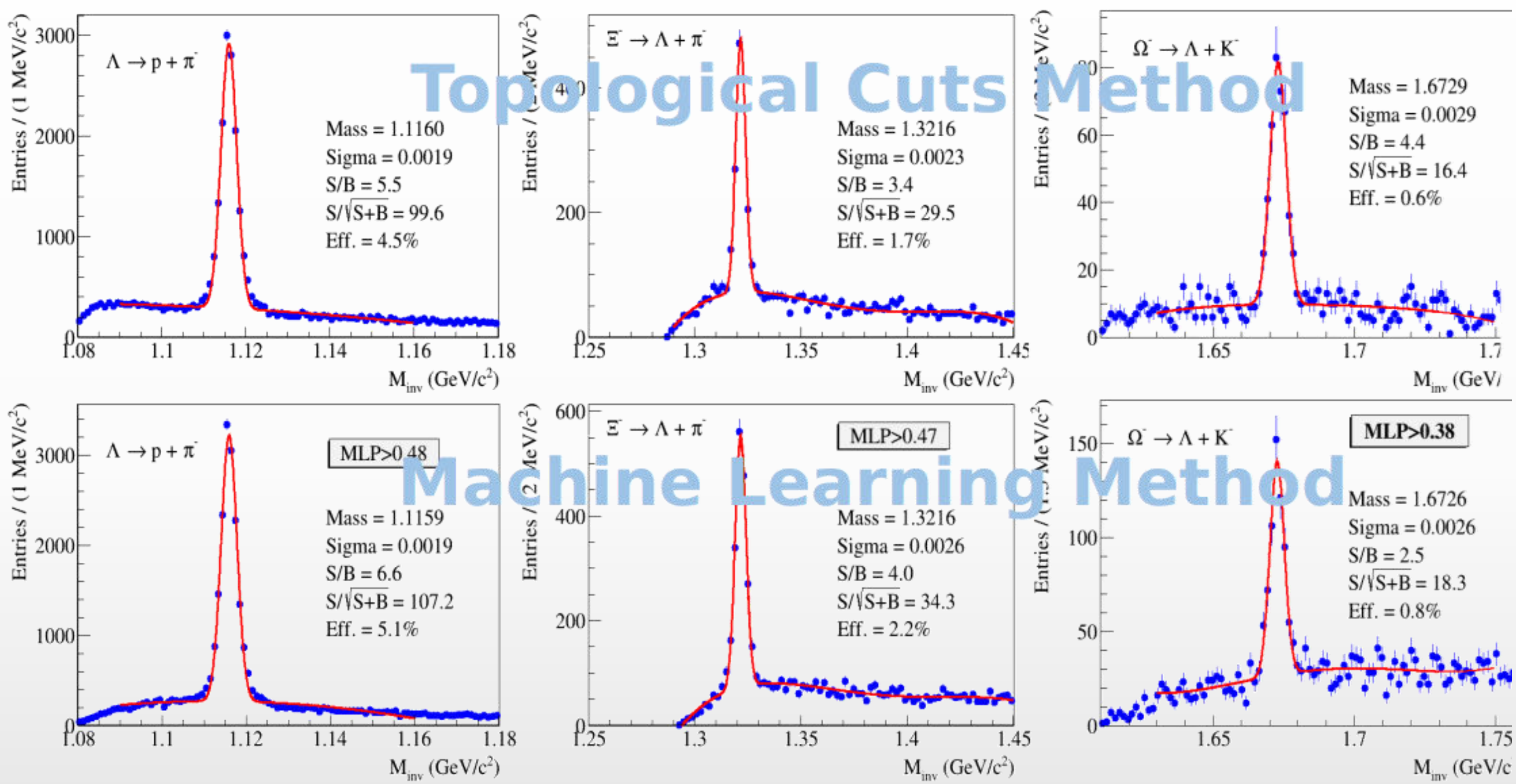

MPD has capabilities to measure production of charged π/K/p, (multi)strange baryons and resonances using charged hadron identification in the TPC&TOF and different decay topology selections

Reconstruction of hypertritons

BiBi@9.2 GeV (PHQMD), 40 M events → full event/detector simulation and reconstruction

Phys.Part.Nucl.Lett. 19 (2022) 1, 46-53

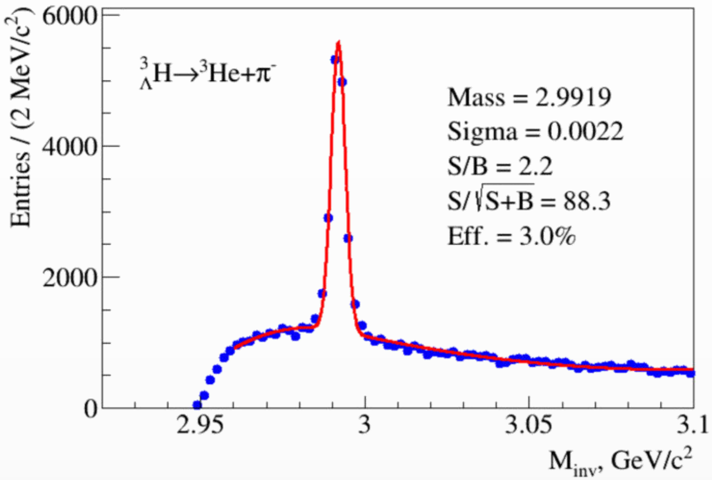

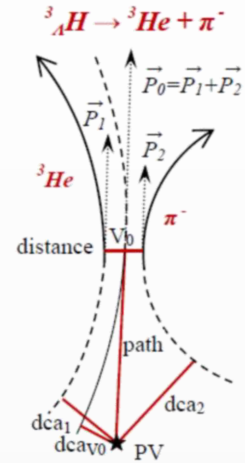

Decay channel	Branching ratio	Decay channel	Branching ratio
$\pi^- + {}^3He$	24.7%	$\pi^- + p + p + n$	1.5%
$\pi^0 + {}^3H$	12.4%	$\pi^0 + n + n + p$	0.8%
$\pi^- + p + d$	36.7%	$d + n$	0.2%
$\pi^0 + n + d$	18.4%	$p + n + n$	1.5%